CARBOXYLATED GRAPHENE OXIDE INTEGRATED CHITOSAN COMPOSITE SCAFFOLDS AS ENCOURAGING MATERIALS FOR TISSUE ENGINEERING

Elena COJOCARU[1], Andra Mihaela ONAȘ[2], Horia IOVU[3]

This work reveals the successful designing of chitosan/carboxyl-modified graphene oxide (CS/GO-COOH) porous composite scaffolds through freeze-drying technique. The main goal of this research was to expand the studies regarding the obtaining of complex structures by chemical interactions between GO-COOH and CS. The scaffolds' structure was characterized through FTIR for confirming the covalent interactions and by Raman to study the disorder degree of GO-COOH sheets. The thermal stability (TGA and DSC), mechanical properties (compressive stress), and morphological analysis (micro-CT) were also examined, in order to consider these porous composite platforms, appropriate for tissue engineering applications.

Keywords: chitosan scaffolds, graphene oxide, composite materials, tissue engineering

1. Introduction

Tissue engineering is a large domain that interplays the studying of the interactions between cell biology, chemistry, and engineering science, by means of maintaining or improving the tissue functions [1]. In the last few decades, the research in tissue engineering field which was based-on innovative solutions for multiple medical diseases, increased exponentially. For designing the appropriate scaffolds for solving medical problems related to tissue engineering, the improvement of biopolymer-based composites is required, being exceptional candidates for biomedical engineering due to their biocompatibility, bioresorptivity, good adsorption properties and antimicrobial activity [2].

Chitosan (CS) is a natural homo-poly-amino-saccharide which is obtained by deacetylation of chitin, resulting from an alkaline treatment. The amino and hydroxyl functionalities from the CS structure contribute to the highly reactive character of this polysaccharide. The free amino groups of CS provide a positive

[1] PhD eng., Advanced Polymer Materials Group, University POLITEHNICA of Bucharest, Romania, e-mail: elena.cojocaru3105@upb.ro
[2] MS eng., Advanced Polymer Materials Group, University POLITEHNICA of Bucharest, Romania, e-mail: andra_mihaela.onas@upb.ro
[3] Prof., Advanced Polymer Materials Group, University POLITEHNICA of Bucharest, Academy of Romanian Scientists, Bucharest, Romania, e-mail: horia.iovu@upb.ro

charge to CS, which enables it to interact with different negatively charged compounds [3,4]. The capability of CS to connect with living tissues of the body, integrate and adapt to biological medium makes it an interesting biomaterial with versatile applications such as drug delivery [5], hydrogels [6], tissue engineering [7]. Its biocompatibility, biodegradability and bio-mineralization place CS as a proper choice for tissue engineering scaffolds. In addition, the similar structure of CS with glycosaminoglycan's allows it to mime the extracellular matrix [8]. CS behaves as scaffold material because it supports the cells adhesion, proliferation and osteoblast differentiation, and the formation of mineralized bone matrix as well [9]. Recent advances in ulcer treatment enabled the development of a CS-collagen blend based-on spongy material loaded with an anti-inflammatory drug. The researchers have found that CS improved this complex construct with adhesive, antibacterial and coagulation properties [10]. Although it is extensively exploited in tissue engineering, the mechanical properties of CS do not satisfy the biomaterials expectations for tissue engineering and therefore CS is mainly used as biopolymer matrix for other materials like carbon allotropes enhancing the final mechanical properties of the CS scaffolds.

Graphene is an allotrope of carbon, constituted by a single streaked sp^2-hybridized carbon atoms sheet, organized in a hexagonal network, with nanometer thicknesses and infinite lateral dimensions [11]. Graphene oxide (GO), containing hydroxyl (-OH), carboxyl (-COOH) and ether (C-O-C) functionalities, is more hydrophilic than pure graphene due to the high oxygen content that allows it to easier dispersion in diverse solvents [12]. Carboxylated-GO (GO-COOH) may be obtained by carboxylation of GO, improving the hydrophilic character compared to that of GO and the carboxyl groups assist in the functionalization of GO-COOH with other materials [13]. According to the literature data, GO appealed an incredible attention because of its exceptional characteristics, such as massive mechanical strength [14], powerful thermal and electrical conductivities [15], exotic opto-electronic properties [16], high surface functionality [17], and pronounced antibacterial activity [18]. Due to the mechanical, electrical and chemical extraordinary characteristics of graphene, graphene-based composite materials exhibit a significant place in biomedical field by contributing to tissue engineering development and one of the most suitable combination of materials is made of CS and graphene. However, because of the lack of organic functionalities, pristine graphene structures may be poorly modified with biomolecules, only non-covalent interactions being established. GO instead, besides exhibiting better dispersibility in aqueous media due to the oxygen functionalities, offers much versatile methods of chemical modification with polysaccharides, proteins or other biomolecules. In this way, GO was able to covalently interact with a versatile range of polymers for electronic applications [19,20], biosensors [21] or wide biomedical usage. Anyway, the oxidizing process

of the graphene may alter some electrical or mechanical properties of the final composite and therefore optimum performances may be obtained by juggling the modification parameters of graphene.

The aim of this study is to create the optimum GO-COOH platform to chemically interact with CS through covalent bonds. Although CS/GO-COOH composites were recently reported in the literature for electrochemical determination of amino acids in milk [22] or environmental applications [23,24], the novelty of this research consists in formation of porous nanocomposites for biomedical applications and for the first time these scaffolds were investigated through microcomputer tomography (micro CT) as potential structural support for tissue engineering. In order to achieve complex CS/GO-COOH structures plenty of carboxyl (-COOH) functionalities need to be formed on the surface of GO through mild chemical conditions. In this way, the negative charge of GO-COOH from carboxyl (COO^-) groups and the cationic character of CS from amino (NH_3^+) groups, will allow to obtain new composite structures by establishing chemical bonds between GO-COOH and CS [25]. In addition, the presence of oxygen in GO molecular structure strengthens its ability to interact with a polymer matrix like CS [26]. Therefore, in this study a new chemical route is approached for the synthesis of complex CS/GO-COOH structures by chemical interactions of GO-COOH with CS using different modified GO-COOH/CS ratios. The final composite scaffolds were characterized through FT-IR spectrometry to confirm the covalent interactions and through Raman spectrometry to study the disorder degree of GO-COOH sheets from the scaffolds' structure. Thermal stability was assessed through TGA and DSC analyses. The mechanical properties were tested by compressive stress tests and micro-CT images were evaluated to investigate the potential application as porous platforms for tissue engineering.

2. Materials and methods

2.1. Materials

Commercial GO-COOH was provided by NanoInnova Technologies (NIT). The other required materials including glacial acetic acid (CH3COOH, with 99.8 – 100.5% purity and molecular weight Mw of 60.05 g/mol) and CS ((C6H11NO4)n, with average Mw and 75-85% deacetylated form) were obtained commercially from Sigma-Aldrich. Only distilled water was used in all the analyses.

2.2. Synthesis of GO-COOH based-on CS scaffolds

Firstly, a stock solution of 0.2 M (v/v) acetic acid was prepared under stirring conditions. From this solution a certain volume was used to prepare a homogeneous polymeric solution of 2% (w/v) CS, under heating at 60°C and stirring conditions for 3 hours, to ensure complete dissolution. Separately,

different amounts of GO-COOH in ratio of 0.1, 0.3, 0.5 and 1% were dispersed in minimum volume of acetic acid solution by ultra-sonication process (70% amplitude, pulse: 10 sec on/ 2 sec off) until homogeneous solutions were formed. 10 mL of CS solution were introduced into previous dispersions of GO-COOH and ultrasonicated approximately 30 minutes, until new homogeneous polymeric solutions were obtained. A control sample was also prepared, without GO-COOH content. Each mixture was casted into a Petri dish and frozen at -20°C for 48 hours and then was lyophilized (freeze-dried) at a pressure of 0.28 bar for another 48 hours (D-37520, Osterode am Harz). Fig. 1 shows the interactions that may occur between the components of the system, as well as the images of the CS/GO-COOH-based on obtained porous composite scaffolds.

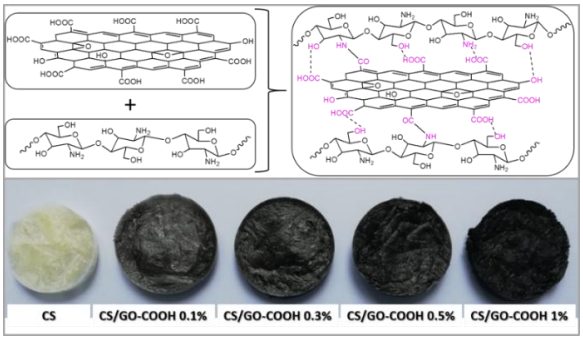

Fig. 1. Schematic model of obtaining the CS/GO-COOH composite porous scaffolds by highlighting the interactions that can occur between the functionalities of the structures and the images of the obtained porous composite scaffolds

2.3. Methods

Fourier Transform Infrared spectrometry (FTIR) spectra were registered on a Bruker Vertex 70 FTIR spectrometer provided with an attenuated total reflectance (ATR) component. The FTIR spectra were recorded using the ATR technique, in 4000 – 600 cm^{-1} wave number range, at a resolution of 4 cm^{-1}, and 32 scans for each sample.

Raman spectra were registered on a Renishaw in Via Raman Microscope. The wavelength of the excitation laser was 785 nm, laser power of about 5% and 3 accumulations for 10 seconds were recorded. The laser beam was concentrated with the 10x objective of the microscope. The Raman spectra were collected in the domain of 3200 – 100 cm^{-1}.

Thermogravimetric analyses (TGA) were done on a Q500 TA instrument, in the temperature range of 25 – 800°C, with a heating rate of 10°C/min in an inert atmosphere of nitrogen, this having a flow rate of 90 mL/min for sample and 10 mL/min for balance. The weight of the samples was in the range of 2-3 mg.

Differential scanning calorimetry (DSC) analyses were done on a Netzsch DSC 204 F1 Phoenix calorimeter using a nitrogen flow rate of 20 mL/min, and a

heating rate of 5°C/min, in the temperature range of ± 20 – 300°C. Each sample of lyophilized scaffold weighted 6 – 7 mg. The weighting of the samples was done in the aluminum pans, then sealed with the caps.

The compressive mechanical studies of the samples were performed using a Universal Testing Machine, Instron 3382 equipment at room temperature. Cylindrical porous scaffolds were used for the tests. All the measurements were achieved in triplicates, the average value was calculated and reported, then the compressive stress (MPa) attributing to each compressive strain (%) was plotted.

Micro computed tomography (μ-CT) was employed to visualize the 3D structure of the samples using a Sky Scan 1272 apparatus. The un-crosslinked porous scaffolds were cut into thin strips of irregular shape and fixed on the holder using modelling paste. The samples were scanned using a voltage of 50 kV and 200 μA as source current. The 3D descriptions were recorded at a pixel size of 1.5 μm, with a rotation step of 0.2° and processed by means of CT NRecon software and reassembled as micrographs of 3D objects using CT-Vox.

3. Results and discussion

3.1. FTIR spectrometry results

FTIR spectrometry was used to investigate the interactions that can appear between CS and GO-COOH at the molecular level. The FTIR spectra were registered for raw materials such as GO-COOH and CS, as well as for final products such CS/GO-COOH 0.1%, 0.3%, 0.5% and 1%, as shown in Fig. 2.

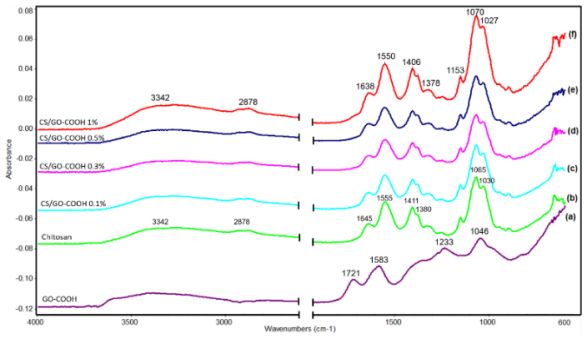

Fig. 2. FTIR spectra of all studied compounds: GO-COOH, chitosan, CS/GO-COOH 0.1%, CS/GO-COOH 0.3%, CS/GO-COOH 0.5% and CS/GO-COOH 1%

The FTIR spectrum of GO-COOH presents characteristic absorption peaks at: 3342 cm^{-1} corresponding to the stretching of hydroxyl group (-OH), 1721 cm^{-1} allocated to the stretching vibration of carbonyl bond (C=O) from carboxyl group, 1583 cm^{-1} attributed to vibrations that correspond to the planar structure of graphene (C=C), 1233 cm^{-1} corresponding to the stretching vibration of ether group C-O-C, and 1046 cm^{-1} which is attributed to the stretching vibration of C–OH band that appears due to the hydroxyl groups of the GO-COOH [27].

CS exhibits characteristic peaks different than those of GO-COOH that will be described as follows. Thus around 3342 cm^{-1} a large band that corresponds to the stretching vibration of hydroxyl (-OH) and amino ($-NH_2$) groups, as well as the intra- and intermolecular hydrogen bonds is observed. The absorption peak at 2878 cm^{-1} may be attributed to symmetric and asymmetric stretching of C-H bond [28]. The peak at 1645 cm^{-1} corresponds to deformational vibration of carbonyl bond (C=O) stretching of amide I and the peak at 1555 cm^{-1} is attributed to N-H bending of amide II [29]. The existence of amides I and II in the CS structure confirms the presence of residual N-acetyl groups, that it is demonstrated by degree of the deacetylation of CS [30]. The peaks at 1411 cm^{-1} and 1380 cm^{-1}, respectively, correspond to $-CH_2-$ bending and $-CH_3$ symmetrical deformations and the peaks at 1065 cm^{-1} and 1030 cm^{-1} can be assigned to stretching vibration of C–O bond [31]. As expected, the chemical grafting reaction occurred after the interaction of carboxyl groups of GO-COOH with the amino groups of CS. The intense signal from 1721 cm^{-1} GO-COOH spectrum assigned to the carboxyl groups is significantly diminished right after the reaction of CS with only 0.1% CS. Increasing the GO-COOH content, it was clearly observed that the peaks from amide I and II (around 1645 cm^{-1} and 1550 cm^{-1}) are found in all composite scaffolds. The FT-IR spectra show not only hydrogen networks and π-π* stacking interactions at the surface of the GO-COOH, but also real covalent amide bonds.

3.2. Raman spectrometry results

Raman spectrometry was used to investigate the chemical modifications of the GO-COOH sheets surface with CS matrix, thus confirming the existence of GO-COOH sheets in CS scaffolds. Fig. 3 exhibits the Raman spectra of pristine GO-COOH and the composite materials with variable concentrations of GO-COOH.

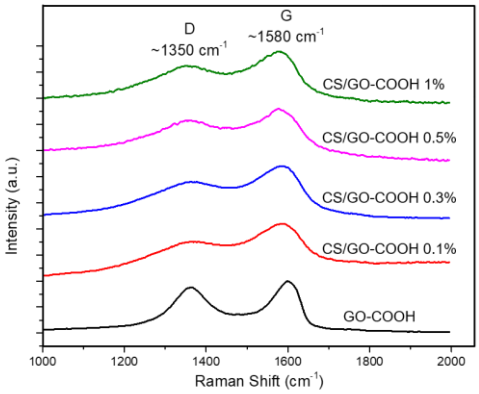

Fig. 3. Raman spectra of pristine GO-COOH and composite scaffolds with 0.1, 0.3, 0.5 and 1 wt% GO-COOH

The Raman spectra of all analyzed materials exhibit two characteristic peaks around 1350 cm^{-1} and 1580 cm^{-1} correlated with the D and G signals,

respectively. The D signal is attributed to the disorders from the GO structure, while the G signal is assigned to ordered mode of sp2-hybridized carbon domains [32]. The ID/IG is used to measure the disorder degree in the GO-COOH sheets resulted as a consequence of the oxidation of graphene layers [33]. Regarding the allure of all spectra, it can be observed that the GO-COOH spectrum contrasts with that of the composite materials through the higher intensity of the D signal, which is attributed to the presence of conformational defects causing from aromatic planar structure, possibly produced from the carboxylation of GO [34].

The ID/IG ratio was determined from the Raman data for each investigated material in order to observe the presence of structural defects comparing to the raw material GO-COOH.

Table 1

Data from Raman Spectrometry regarding the composite scaffolds

Sample	I_D/I_G [785 nm]
CS/GO-COOH 0.1%	0.66
CS/GO-COOH 0.3%	0.69
CS/GO-COOH 0.5%	0.77
CS/GO-COOH 1%	0.73
GO-COOH	0.88

According to the Table 1, the ID/IG ratio in the GO-COOH is found to be 0.88. The ID/IG ratio is significantly decreasing to 0.66 when 0.1% GO-COOH is interacting with CS showing that new GO layers' rearrangement occurs during the process due to the hydrogen and new amide bonds that are formed. Increasing the GO-COOH content, the tendency of GO layers to stack is diminished as observed from the Raman data. Therefore, the conjugation of the π electrons from planar structure of the GO-COOH is perturbed by the non-covalent physical interactions that occur between CS and GO-COOH sheet surface. At the highest content of GO-COOH the ID/IG ratio is 0.73, but the highest exfoliation is obtained when 0.5% GO-COOH was used. These results may occur due to the tendency of the GO-COOH layers to agglomerate at higher concentrations hindering the dispersion of the GO-COOH sheets within the CS matrix.

3.3. TGA results

The thermal stability of both the raw materials and composite scaffolds was evaluated through TGA analysis aiming to investigate the intermolecular interactions and thermal comportment of CS/GO-COOH-based materials. The TGA curves for each investigated material are shown in Fig. 4.

The degradation of raw CS take place in three stages. In the first step, in the temperature interval of 30 – 110°C the evaporation of adsorbed moisture from CS sample occurs. The second step, in the range of temperature 110 – 300°C two

important weight losses are showed that indicate the deacetylation of CS and elimination of volatile products, followed by the thermal degradation (240 – 270°C) [35].

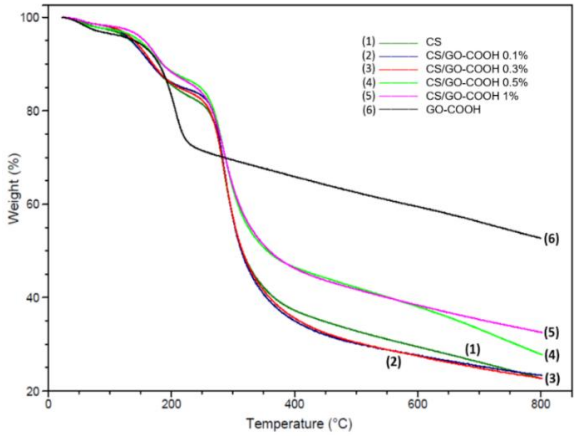

Fig. 4. TGA curves of all studied compounds

From Fig. 4 it may be observed that the highest thermal stability is shown by GO-COOH which exhibits two important degradation stages: below 100°C corresponding to the evaporation of moisture entrapped in the graphene stacking, and second degradation stage around 200°C attributed to the degradation of oxygen functionalities, especially -COOH groups. After the incorporation of the GO-COOH in the CS matrix the thermal stability of the final compounds is obviously increased. As expected, by increasing the GO-COOH content the yield of transformation into -NH-C=O- bonds is higher, therefore ample intermolecular networks are created increasing the thermostability in comparison to pure CS. The temperature values corresponding to 3, 5 and 10% weight loss and total weight loss in the range of 25 – 800°C of the all studied samples, are summarized in Table 2.

Table 2

Thermal properties of samples analyzed from TGA [25-800°C]

Sample	T_d 3 % (°C)	T_d 5 % (°C)	T_d 10 % (°C)	Total weight loss (%)
CS	108	134	168	77
CS/GO-COOH 0.1%	116	135	167	77
CS/GO-COOH 0.3%	120	140	170	77
CS/GO-COOH 0.5%	119	149	185	72
CS/GO-COOH 1%	135	157	186	67
GO-COOH	83	141	180	51

3.4. DSC results

The thermal behavior of raw materials and composite scaffolds was evaluated using DSC analysis. The registered DSC curves for each sample and the main thermal parameters (the dehydration, glass transition and degradation temperatures) are shown in Fig. 5 and Table 3, respectively.

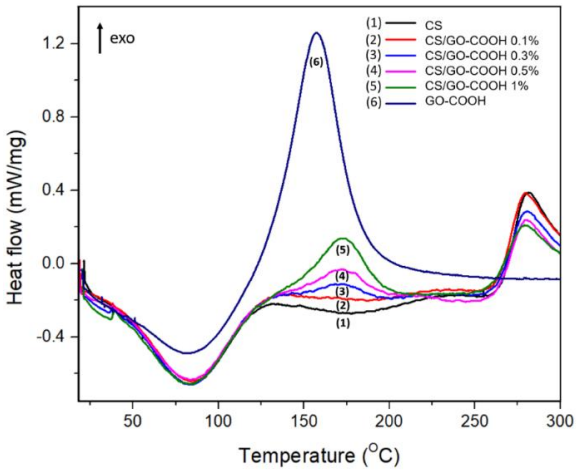

Fig. 5. DSC curves of CS, GO-COOH and composite scaffolds with different % of GO-COOH

Table 3

Thermal properties of samples analyzed from DSC

Sample	$T_{dehydration}$ (°C)	T_g (°C)	$T_{degradation}$ (°C)
CS	83	178	282
CS/GO-COOH 0.1%	83	187	280
CS/GO-COOH 0.3%	85	173	281
CS/GO-COOH 0.5%	83	172	280
CS/GO-COOH 1%	84	174	279
GO-COOH	82	-	157

DSC curve of pure CS indicates three representative peaks: the first endothermic peak at about 83°C is attributed to the loss moisture due to the hydrophilic groups of CS, the second broad endothermic peak at about 178°C indicating the glass transition temperature (Tg) of CS and the third peak that appears at 282°C corresponding to the CS's thermal degradation. In case of GO-COOH, the DSC curve presents an endothermic peak at 82°C caused by the dehydration process and a pronounced exothermic peak around 157°C which is assigned to the degradation of -COOH and -OH functional groups from the GO-COOH surface. Concerning the composite scaffolds, regardless the amount of GO-COOH added, no significant changes in the dehydration and degradation temperature of the composites were observed compared to pure CS. However, the

strong exothermic peak of GO-COOH was extremely reduced after the functionalization with CS demonstrating that the -COOH groups were consumed during the interactions with $–NH_2$ groups of CS. A slight decrease in the thermal stability of CS/GO-COOH composites, noticed in DSC thermograms by a shift of the Tg towards lower values was observed.

3.5. Compressive studies result

The mechanical behavior of all un-crosslinked porous composite scaffolds with various GO-COOH amounts was examined by compressive tests at ambient temperature (average values of three measurements per sample) and the results are summarized in the Table 4. The representative compressive stress versus compressive strain curves are shown in Fig. 6. It is important to mention that the compressive studies were performed in agreement with the European Standard EN ISO 604: 2003, namely "Determination of compressive properties".

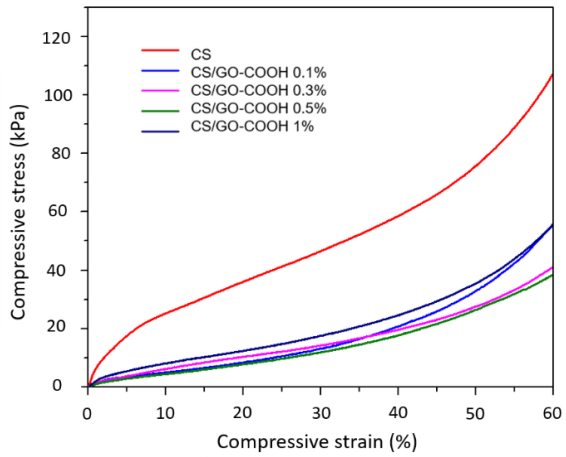

Fig. 6. Compressive tests of all composite scaffolds

Table 4

Mechanical properties of samples analyzed by compressive test

Sample	Compressive stress (kPa)	
	30%	60%
CS	46.5	107.6
CS/GO-COOH 0.1%	13.1	56.0
CS/GO-COOH 0.3%	14.3	41.3
CS/GO-COOH 0.5%	11.9	38.6
CS/GO-COOH 1%	17.6	56.0

It can be noticed a decrease of mechanical properties for the composite porous scaffolds compared with pure CS scaffold. This can be justified by the following aspects: non-crosslinking of scaffolds and increasing the disorder in

structures with increasing the graphene content, according to Raman data. It may be seen the differences between CS scaffold and composite scaffolds regarding to compressive stress at 30% and 60% compressive strain, in Table 4. These decreases of mechanical properties of the composite porous scaffolds may be attributed to the formation of graphene layers' agglomerates, as will be seen from the micro-CT analysis, which destroy the structure of the polymeric matrix, and the macromolecules' disorganization disrupt the formation of solid networks with increased mechanical strength.

3.6. Micro-CT scanning results

Micro-CT scanning technique has the role to exhibit the 3D internal structure of the samples. The morphology of scaffolds was characterized by micro-CT scanner, and CT-images are shown in Fig. 7. Using this method, the pure CS scaffold and composite scaffold with 1% GO-COOH (CS/GO-COOH 1%) were scanned. Then the images were processed and reassembled as micrographs of 3D object.

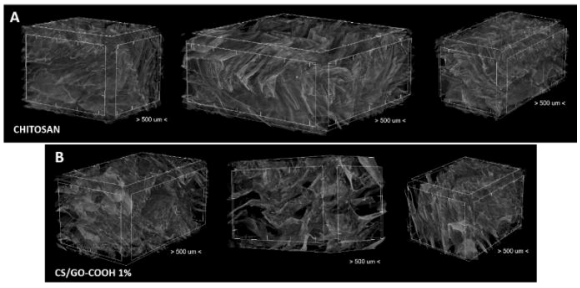

Fig. 7. 3D micro-CT micrographs of their cross-section. A: micro-CT images of the CS scaffolds; B: micro-CT images of the CS/GO-COOH 1% composite scaffolds. The scale bar is 500 μm for both panels (A and B).

As it is demonstrated, the scaffolds with porous architecture exhibit special advantages that make them suitable for tissue engineering. The scaffolds provide structural support to ensure the cells attachment, proliferation and differentiation. Also, the literature studies show that the porosity and pore interconnectivity are characteristic points in a scaffolds structure [36].

Micro-CT images of the CS scaffolds (Fig. 7A) show a dense porous structure with a smoother surface of CS sheets, while the composite scaffold with GO-COOH 1% (Fig. 7B) exhibits a rarefied structure in which it can see empty spaces between material sheets. Moreover, the sheet's surface is more wrinkled than that of the CS sheets. On the surface of the rarefied composite scaffold, small loads and agglomerations of GO-COOH can be observed, due to the hydrogen bonds, which are formed between -OH and $–NH_2$ groups from CS and -COOH functionalities of GO-COOH. These results are in agreement with compressive

studies and Raman data which show disorder in the structure of the composite scaffolds containing GO-COOH.

4. Conclusions

All the results presented in this study reveal the successful synthesis and designing of CS/GO-COOH porous scaffolds obtained through freeze-drying technique. Composite scaffolds were achieved by incorporation the GO-COOH into the CS-based polymeric matrix.

The porous structure promotes the development of tissues on such platforms, through the migration, growth, and differentiation of living cells. Therefore, by micro-CT analysis it was shown the porous morphology of the scanned scaffolds. Through FTIR spectrometry was exposed both the formation of hydrogen bonds, as well as the formation of amide bonds between the -COOH groups of GO-COOH and the $-NH_2$ groups of CS. Raman spectrometry was employed to study the degree of disorder in the GO-COOH-containing composite structures. The thermal stability, highlighted by the changes at the molecular level, was evaluated by TGA and DSC analyses. The TGA results shows that after the insertion of GO-COOH into the CS matrix, the thermal stability of the final compounds is increased. From the DSC thermograms, the reduction of the sharp exothermic peak of GO-COOH in composite scaffolds was demonstrated that the -COOH groups were consumed during the covalent interactions with $-NH_2$ groups of CS.

Hence, the design of optimum GO-COOH platform that chemically interacts with CS matrix through covalent bonds, forming a complex CS/GO-COOH structures with porous architecture, was successfully realized through freeze-drying method, and can be suitable for applications in tissue engineering.

R E F E R E N C E S

[1]. *S. Levenberg, A. Khademhosseini, R. Langer*, Chapter 37 – Embryonic stem cells in tissue engineering, Handbook of Stem Cells (Second Edition), **vol. 1**, 2013, 427-437

[2]. *C. K. Chou, S. M. Chen, Y. C. Li, T. C. Huang, J. A. Lee*, SpringerPlus, **vol. 4,** no. 1, 2015, 1-7

[3]. *O. Felt, P. Buri, R. Gurny*, Chitosan: a unique polysaccharide for drug delivery, Drug Dev. Ind. Pharm. **vol. 24,** no. 11, 1998, 979-993

[4]. *S. Islam, M. A. Rahman Bhuiyan, M. N. Islam*, Chitin and Chitosan: Structure, Properties and Applications in Biomedical Engineering, J Polym Environ, Springer Science+Business Media New York, 2016

[5]. *J. Lizardi-Mendoza, W. M. Argüelles Monal, F. M. Goycoolea Valencia*, Chapter 1 – Chemical Characteristics and Functional Properties of Chitosan, Chitosan in the Preservation of Agricultural Commodities, 2016, 3-31

[6]. *M. Rodrıguez-Vazquez, B. Vega-Ruiz, R. Ramos-Zuniga, D. A. Saldana-Koppel, L. F. Quinones-Olvera*, Chitosan and its potential use as a scaffold for tissue engineering in regenerative medicine, BioMed Res. Int., 2015, 1-15

[7]. *M. Kumar, A. Brar, V. Vivekanand, N. Pareek*, Possibilities and perspectives of chitosan scaffolds and composites for tissue engineering, Chapter 7, Materials for Biomedical Engineering, Nanobiomaterials in Tissue Engineering, 2019, 167-203

[8]. A. *Tchobanian, H. Van Oosterwyck, P. Fardim*, Polysaccharides for tissue engineering: Current landscape and future prospects, Carbohydrate Polymers, **vol. 205**, 2019, 601-625

[9]. *S. Ranganathan, K. Balagangadharan, N. Selvamurugan*, Chitosan and gelatin-based electrospun fibers for bone tissue engineering – review, International Journal of Biological Macromolecules, **vol. 133**, 2019, 354-364

[10]. *A. Alagha, A. Nourallah, S. Hariri*, Characterization of dexamethasone loaded collagen-chitosan sponge and in vitro release study, Journal of Drug Delivery Science and Technology, **vol. 55**, 2020, 101449

[11]. *E. I. Biru, H. Iovu*, Graphene nanocomposites studied by Raman spectroscopy, Raman Spectroscopy, IntechOpen, 2018, 179-201

[12]. *W. Gao*, Graphene Oxide – Reduction Recipes, Spectroscopy, and Applications, Springer, ISBN 978-3-319-15499-2, DOI 10.1007/978-3-319-15500-5

[13]. *S. Yu, J. Liu, W. Zhu, Z.-T. Hu, T.-T. Lim, X. Yan*, Facile room-temperature synthesis of carboxylated graphene oxide copper sulfide nanocomposite with high photodegradation and disinfection activities under solar light irradiation, Scientific Reports, **vol. 5**, no.1, 2015

[14]. *C. Lee, X. Wei, J.W. Kysar, J. Hone*, Measurement of the elastic properties and intrinsic strength of monolayer graphene, Science, **vol. 321**, 2008, 385-388

[15]. A. *A. Balandin, S. Ghosh, W. Bao, I. Calizo, D. Teweldebrhan, F. Miao, et al.*, Superior thermal conductivity of single-layer graphene, Nano Lett. **vol. 8**, 2008, 902-907

[16]. *G. Eda, G. Fanchini, M. Chhowalla*, Large-area ultrathin films of reduced graphene oxide as a transparent and flexible electronic material, Nat. Nanotechnol. **vol. 3**, 2008, 270-274

[17]. *E. I. Biru, S. A. Garea, H. Iovu*, Developing polybenzoxazine composites based on various carbon structures, Macromol. Chem. Phys. **vol. 220**, 2019, 1800322

[18]. *A. J. Ryan, C. J. Kearney, N. Shen, U. Khan, A.G. Kelly, C. Probst, et al.*, Electroconductive biohybrid collagen/pristine graphene composite biomaterials with enhanced biological activity, Adv. Mater. **vol. 30**, 2018, 1706442

[19]. *E. I. Biru, S. A. Garea, A. Nicolescu, E. Vasile, H. Iovu*, Advanced polybenzoxazine structures based on modified reduced graphene oxide, Polymers, **vol. 10**, 2018, 941

[20]. *I. Biru, C. M. Damian, S. A. Garea, H. Iovu*, Benzoxazine-functionalized graphene oxide for synthesis of new nanocomposites, European Polymer Journal, **vol. 83**, 2016, 244-255

[21]. *Lee, J. Kim, S. Kim, D. H. Min*, Biosensors based on graphene oxide and its biomedical application, Advanced Drug Delivery Reviews, **vol. 105**, 2016, 275-287

[22]. *E. Fooladi, B. M. Razavizadeh, M. Noori, S. Kakooei*, Application of carboxylic acid- functionalized of graphene oxide for electrochemical simultaneous determination of tryptophan and tyrosine in milk, SN Applied Sciences, **vol. 2**, no.527, 2020

[23]. *L. Zhao, S. Yang, A. Yilihamu, Q. Ma, M. Shi, B. Ouyang, Q. Zhang, X. Guan, S.-T. Yang*, Adsorptive decontamination of Cu2+-contaminated water and soil by carboxylated graphene oxide/chitosan/cellulose composite beads, Environmental Research, **vol. 179**, 2019, 108779

[24]. *L. Zhao, X. Guan, B. Yu, N. Ding, X. Liu, Q. Ma, S. Yang, A. Yilihamu, S.-T. Yang*, Carboxylated graphene oxide-chitosan spheres immobilize Cu2+ in soil and reduce its bioaccumulation in wheat plants, Environmental International, **vol. 133**, 2019, 105208

[25]. A. *Singh, G. Sinsinbar, M. Choudhary, V. Kumar, R. Pasricha, H. N. Verma, S. P. Singh, K. Arora,* Graphene oxide-chitosan nanocomposite based electrochemical DNA biosensor for detection of typhoid, Sensors and Actuators B: Chemical, **vol. 185**, 2013, 675-684

[26]. *Kosowska, P. Domalik-Pyzik, M. Nocuń, J. Chłopek*, Chitosan and graphene oxide/reduced graphene oxide hybrid nanocomposites – Evaluation of physicochemical properties, Materials Chemistry and Physics, **vol. 216**, 2018, 28-36

[27]. *D. He, Z. Peng, W. Gong, Y. Luo, P. Zhao, L. Kong*, Mechanism of a green graphene oxide reduction with reusable potassium carbonate, Royal Society of Chemistry, **vol. 5**, 2015, 11966

[28]. *G. Cardenas, S. P. Miranda*, FTIR and TGA studies of chitosan composite films, Journal of the Chilean Chemical Society, **vol. 49**, no. 4, 2004, 291-295

[29]. *J. Ghitman, R. Stan, S. Cecoltan, M. C. Chifiriuc, H. Iovu*, Hybrid nanocarriers based on PLGA-vegetable oil: A novel approach for high lipophilic drug delivery. Journal of Drug Delivery Science and Technology, **vol. 46**, 2018, 162-172

[30]. *B. Krishnaveni, R. Ragunathan*, Extraction and Characterization of Chitin and Chitosan from F. solani CBNR BKRR, Synthesis of their Bionanocomposites and Study of their Productive Application, Journal of Pharmaceutical Sciences and Research, **vol. 7**, no. 4, 2015, 197-205

[31]. *F. Queiroz, K. R. T. Melo, D. Araujo Sabry, G. Lanzi Sassaki, H. A. Oliveira Rocha*, Does the use of chitosan contribute to oxalate kidney stone formation? Marine Drugs, **vol. 13**, 2015, 141-158

[32]. *A. M. Pandele, C. Andronescu, E. Vasile, I. C. Radu, P. Stanescu, H. Iovu*, Non-covalent functionalization of GO for improved mechanical performances of pectin composite films, Composites Part A: Applied Science and Manufacturing, **vol. 103**, 2017, 188-195

[33]. *J. Nath, A. Chowdhury, S. K. Dolui*, Chitosan/graphene oxide- based multifunctional pH-responsive hydrogel with significant mechanical strength, self-healing property, and shape memory effect, Adv. Polym. Technol. **vol. 37**, Wiley Periodicals 2018, 3665-3679

[34]. *J. Chen, X. Zhang, H. Cai, Z. Chen, T. Wang, L. Jia, J. Wang, Q. Wan, X. Pei*, Osteogenic activity and antibacterial effect of zinc oxide/carboxylated graphene oxide nanocomposites: preparation and in vitro evaluation, Colloids and Surfaces B: Biointerfaces, **vol. 147**, 2016, 397-407

[35]. *B. A. Howell, M. R. Alomari, A. Dumitrascu, R. S. Opperman*, Properties of the Phosphoramide Derived from Chitosan and 9,10-Dihydro-9-oxa-10-phosphaphenanthrene-10-oxide, 2015

[36]. *Q. L. Loh, C. Choong*, Three-dimensional scaffolds for tissue engineering applications: Role of porosity and pore size, Tissue Engineering Part B: Reviews, **vol. 19,** no. 6, 2013, 485-502